Fission of heavy nuclei induced by stopped antiprotons. II. Correlations between fission fragments

Y. S. Kim,[1,*] A. S. Iljinov,[2] M. V. Mebel,[2] P. Hofmann,[1,†] H. Daniel,[1] T. von Egidy,[1] T. Haninger,[1] F. J. Hartmann,[1] H. Machner,[3] H. S. Plendl,[4] and G. Riepe[3]

[1]*Physik-Department, Technische Universität München, D-85748 Garching, Germany*

[2]*Institute for Nuclear Research, Russian Academy of Sciences, 117312 Moscow, Russia*

[3]*Forschungszentrum Jülich, D-52425 Jülich, Germany*

[4]*Florida State University, Tallahassee, Florida 32306*

(Received 12 February 1996)

Antiproton-induced fission has been investigated with a novel double-arm fission fragment spectrometer. The correlations in mass, energy, and velocity between two fragments were measured. The dependence of total kinetic energy, velocity, momentum of the fissioning nucleus, and momentum of the fission fragments on the mass loss was deduced and analyzed in the framework of the dynamical statistical model. This model takes into account all stages before, during and after $\bar{p}$-induced fission (atomic cascade, intranuclear cascade, evaporation cascade, fission of the compound nucleus, evaporation from the fission fragments). The mass loss was used as a measure of the excitation energy to classify the fission events according to the corresponding excitation energies. Some discrepancies between the model calculation and the experiment show the important role of dissipative effects in the $\bar{p}$-induced fission process. [S0556-2813(96)04511-6]

PACS number(s): 25.43.+t, 24.75.+i, 25.85.Ge

I. INTRODUCTION

Related to the investigation of nuclear matter at high excitation energy E^* there is an increasing interest in high energy fission. The fission phenomenon is like a microscope through which we can have a close look at the nature and behavior of hot nuclear matter. One very good example is the study of fission time which gives us a clue to dissipative effects in fission [1]. Some authors have tried to search for exotic nuclear phenomena such as fireballs [2] or cleavage of the nucleus [3] by measuring correlated fission fragments, while others tried to learn about multifragmentation by looking at the total-mass–total-kinetic-energy correlation of coincident fragments [4]. In this respect the antiproton- ($\bar{p}$-) induced fission is very interesting because it produces not only another set of fission data but it can also shed some light on the $\bar{p}$-nucleus interaction, which is quite different from conventional nuclear reactions.

The first part of our publication [5] dealt with the general aspects of fission induced by stopped antiprotons by comparing the inclusive experimental spectra with model calculations for four sequential processes: the atomic cascade, the intranuclear cascade (INC), the decay of the compound nucleus (simulated with the statistical evaporation model), and the fission process (simulated with a diffusion model based on the Fokker-Planck equation). The double-arm fission fragment spectrometer with which we measured two masses, two kinetic energies, and the folding angle between the fission fragments is explained elsewhere [6]. The spectrometer was employed at LEAR/CERN to measure the fission fragments resulting from $\bar{p}$ annihilation in ^{238}U, ^{232}Th, and ^{209}Bi targets.

In the present paper we will examine various correlations between mass, energy, and velocity of coincident fission fragments from $\bar{p}$-induced fission which has properties different from those of heavy-ion-induced fission: Only very little linear and angular momenta are involved. Such correlations can provide information on both $\bar{p}$ annihilation and subsequent evaporation and/or fission processes. The mass loss Δm (the target mass minus the mass sum of the two coincident fragments after all evaporation processes) will be used as a measure for the excitation energy of the compound nucleus right after the fast cascade process. This procedure will be justified later. This experimental observable is very useful since it enables us to classify each single fission event according to its excitation energy.

Recently some evidence arose from heavy-ion-induced fission experiments that the fission process is so strongly overdamped that the fissioning nucleus is almost cold at the time of scission [7]. A direct measurement of such an effect in the case of $\bar{p}$-induced fission would be desirable, because only little angular momentum is involved. The common experimental method to study such an effect is to measure neutron spectra at various angles with respect to the fission axis and to deconvolute the spectra to obtain the neutron multiplicity before and after scission. Apart from this technique the correlation between the total kinetic energy (TKE) and the mass loss can also provide a means to observe the effect, since particle evaporation before and after fission has different consequences on the fission kinematics.

II. INC, EVAPORATION, AND FISSION CALCULATIONS

The calculation of the intranuclear cascade and the subsequent evaporation and fission is described in detail in the first part of our publication [5]. Here only some results will be

*Present address: Korea Institute of Geology, Mining and Materials, Taejon, South Korea.

†Deceased.

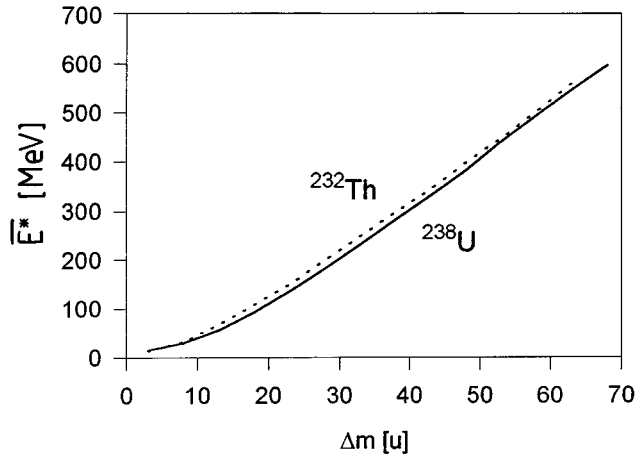

FIG. 1. Result of a model calculation for the average excitation energy $\overline{E^*}$ as a function of the mass loss Δm. The slopes of the graphs imply that $\Delta m = 1$ roughly corresponds to $E^* = 10$ MeV.

shown. First of all, the correlation between average excitation energy E^* and mass loss Δm is shown in Fig. 1. Δm is given by $\Delta m = A_t - 1 - M_{\rm tot}$, with A_t the number of nucleons in the target nucleus and $M_{\rm tot}$ the total number of nucleons in both fission fragments. At $\Delta m > 10$, E^* depends almost linearly on Δm for both U and Th. This kind of correlation was first used in the work of Remsberg *et al.* [8] who combined the results of the two early pioneering works by Metropolis *et al.* [9] and by Dostrovsky *et al.* [10]. The slope of 10 MeV/(emitted nucleon) is the same Remsberg *et al.* had obtained. Hence it is justified to use Δm as a measure of E^* with a conversion factor of 10 MeV/(emitted nucleon). Figure 2 shows the number of protons and neutrons emitted during the cascade as a function of the mass loss and, consequently, of E^*. There is practically no difference in the slope for U and Th, and a linear relationship holds between the number Δn of cascade nucleons and Δm: $\Delta n/\Delta m = 0.14$ for neutrons, $\Delta n/\Delta m = 0.06$ for protons, and thus $\Delta n/\Delta m = 0.20$ for cascade *nucleons*. This leads to 50 MeV per cascade nucleon, which is the same value Metropolis *et al.* had obtained. The number of nucleons evaporated from the compound nucleus before fission is shown in Fig. 3 as a function of Δm. Some small substructure in the curves is due to the statistics of the calculation. The number of evaporated neutrons increases with increasing Δm until $\Delta m = 18$ ($E^* \approx 100$ MeV; cf. Fig. 1) and then drops slowly with increasing Δm. It is remarkable that neutron evaporation is not a dominant decay channel at $\Delta m > 30$, i.e., $E^* > 220$ MeV. Proton evaporation is highly suppressed because of the rather high Coulomb barrier and contributes only very little. The emission of α particles, however, is important for the mass loss during evaporation before scission. Charged particles carry away the largest part of the mass of the hot compound nucleus because their binding energy for neutron-deficient compound nuclei may become even negative (fission fragments, neutron-rich nuclei, emit predominantly neutrons). As a result of the competition with the emission of other particles, the number of prescission neutrons does not increase with the excitation energy E^* of the compound nucleus (i.e., with the decrease of the total mass $M_{\rm tot}$), as was observed in

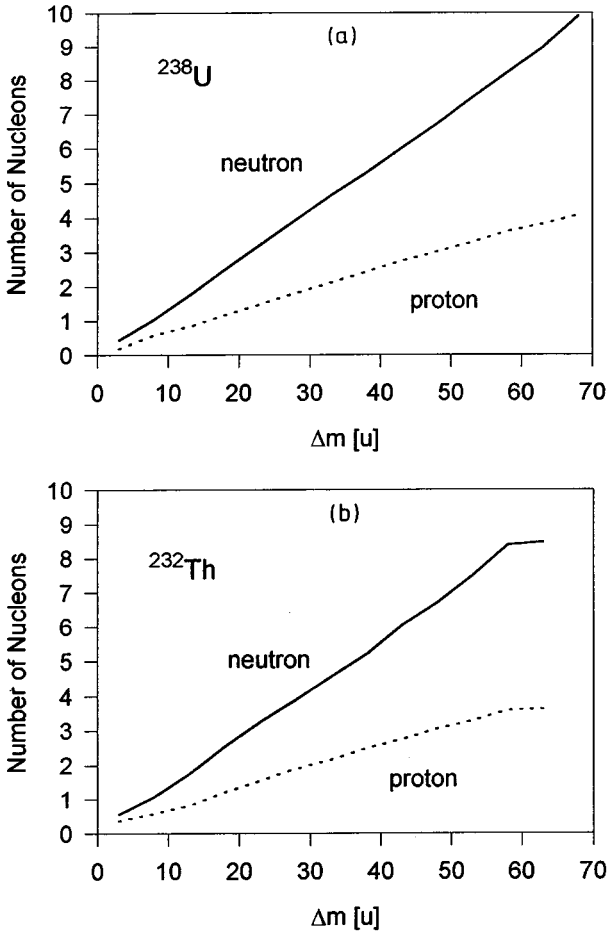

FIG. 2. Result of a model calculation for the average number of cascade protons (dotted lines) and neutrons (solid lines) as a function of Δm, (a) for ^{238}U and (b) for ^{232}Th. Adding protons and neutrons gives 0.2 nucleon/Δm, which corresponds to 50 MeV per cascade nucleon.

heavy-ion experiments [7]. Hence the mass loss in fission of hot nuclei may not be identified with the neutron multiplicity, as is often done. Again, there is no large difference in the gross feature between U and Th, except that the neutron evaporation saturates at $\Delta m \approx 22$ for Th. It has to be kept in mind that the above-mentioned relations are the results of our calculations.

It is instructive to see the change of TKE due to various particle evaporations. The simple liquid drop model [11] predicts the $\overline{\rm TKE}^*$ (total kinetic energy of two fission fragments after full acceleration assuming no evaporation from the fragments) to be

$$\overline{\rm TKE}^* = 0.124\, Z^2/M_{\rm tot}^{*\,1/3}\ {\rm MeV}, \tag{1}$$

where Z and the mass $M_{\rm tot}^*$ are the charge and mass of the fissioning nucleus, respectively. The average total kinetic energy that can be compared with the experiment is the value *after* all evaporations which can be approximated by

$$\overline{\rm TKE} = \overline{\rm TKE}^* \frac{M_{\rm tot}}{M_{\rm tot}{}^*}, \tag{2}$$

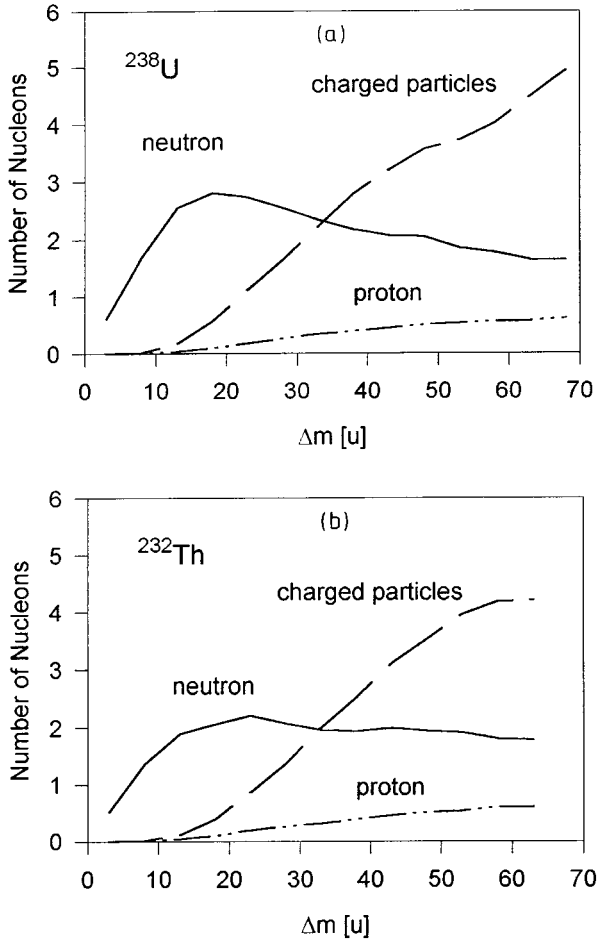

FIG. 3. Result of a model calculation for the average number of evaporated protons (double-dot-dashed lines), neutrons (solid lines), and other charged particles (dashed lines) as a function of Δm (a) for ^{238}U and (b) for ^{232}Th. The ordinate gives the number of nucleons. From $E^* \approx 300$ MeV upward neutron evaporation is no longer the dominant decay channel.

where $M_{\rm tot}$ is the sum of the masses of the two fragments after all evaporations are finished. Now the change of $\overline{\rm TKE}$ per evaporated nucleon $d\overline{\rm TKE}/dM_{\rm tot}$ can be obtained from Eqs. (1) and (2) for various evaporated particles in the case of $^{238}_{92}$U as function of $Z/M_{\rm tot}$ as shown in Fig. 4(a). The $d\overline{\rm TKE}/dM_{\rm tot}$ for prescission neutrons, protons, α particles, and postscission neutrons are about 0.4, -3, -1.4, and -0.7 MeV/nucleon, respectively. Note that only prescission neutron evaporation increases the TKE.

It may be even more instructive to see the change of the fragment velocities due to the particle evaporations because the postscission evaporation will, on average, not affect the velocity, enabling us to observe rather purely the effect of prescission evaporations. We introduce the root mean square velocity of the two fragments as

$$v_{\rm rms} = \sqrt{v_1\, v_2}. \tag{3}$$

From the fission kinematics one obtains

$$\mathrm{TKE}^* = \frac{M^*_{\rm tot}}{2}\, v_1\, v_2. \tag{4}$$

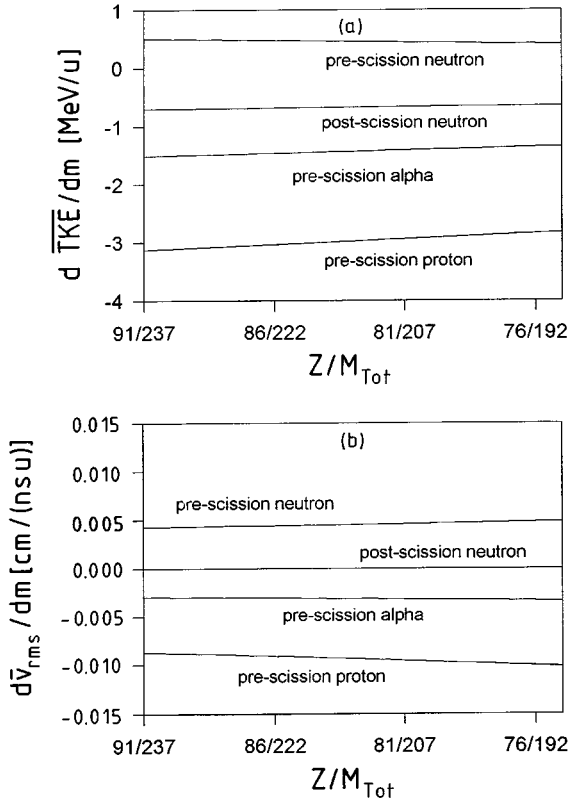

FIG. 4. The slope of (a) $\overline{\rm TKE}$ and (b) $\overline{v}_{\rm rms}$ as a function of particle evaporation before and after scission versus Z/A. The values were calculated with Eqs. (1), (2), and (5). Charge and mass of the fissioning nucleus were arbitrarily selected approximately following the line of β stability in the nuclide chart.

From Eqs. (1), (3), and (4) and assuming $\mathrm{TKE}^* \approx \overline{\rm TKE}^*$ as well as $v_{\rm rms} \approx \overline{v}_{\rm rms}$, it follows, for the case of the most probable mass and charge of the fragments,

$$\overline{v}_{\rm rms} = \left(0.248 \frac{Z^2}{M_{\rm tot}{}^{*4/3}}\right)^{1/2}. \tag{5}$$

Based on Eq. (5), we can also obtain $\overline{v}_{\rm rms}$ for various charges and masses of the fissioning nuclei. The role of particle evaporation on $v_{\rm rms}$ calculated in this way is shown in Fig. 4(b). The major difference from Fig. 4(a) is that the postscission particle emission has no effect on $\overline{v}_{\rm rms}$. The $d\overline{v}_{\rm rms}/dM_{\rm tot}$ values for prescission neutrons, protons, and α particles are calculated to be about 0.004, -0.09, and -0.003 cm/(ns nucleon), respectively.

The importance of these calculated $d\,\overline{\rm TKE}/dM_{\rm tot}$ and $d\overline{v}_{\rm rms}/dM_{\rm tot}$ values is obvious: In the $(2E,2v)$ correlation measurement, one obtains the correlation of TKE and velocity to the mass loss Δm, and the slopes at each given Δm in those correlations can be interpreted as the consequence of the various particle evaporations before or after scission. Such a correlation can, therefore, reveal some information on prescission and postscission particle evaporations as will be shown in Sec. III D.

III. DISCUSSION AND COMPARISON OF EXPERIMENTAL AND CALCULATED CORRELATIONS BETWEEN FISSION FRAGMENTS

A. Experiments

Our double-energy double-time-of-flight experiment was performed with a double-arm fission fragment spectrometer consisting of two *p-i-n* diode arrays (with 144 diodes each) using U, Th, and Bi targets. The experimental details are explained elsewhere [6]. With the spectrometer it is possible to obtain the masses (M_1,M_2), kinetic energies (E_1,E_2), and velocities (v_1,v_2) of and the folding angle (Θ_f) between two coincident fragments and to determine correlations between mass, kinetic energy, velocity, and momentum. Mass, energy, and time resolution were about 8 nucleon, 2 MeV, and 1.5 ns full width at half maximum (FWHM), respectively. The number of registered coincident fission events is 17 000, 4000, and 420 for U, Th, and Bi, respectively. One should take the different number of events into account when comparing correlations among different targets because scatter plots do not show the real width of the distributions. The inclusive single distributions have already been shown in our previous paper [5].

B. Correlations between mass, energy, and velocity of coincident fission fragments

Figure 5 shows the correlation between the two fragment masses. The events with mass <25 are not included in the plots and the events are not corrected for the efficiency of the spectrometer. If they were corrected, the center of the distributions would move slightly to lower masses in the cases of U and Th, and somewhat more in the case of Bi because the average folding angle for Bi is larger than that for U and the counting efficiency decreases with increasing folding angle. The total mass $M_{\rm tot}$ can be obtained just by $M_{\rm tot} = m_1 + m_2$. The points beyond $M_{\rm tot} = 237$ for U, $M_{\rm tot} = 231$ for Th, and $M_{\rm tot} = 208$ for Bi — one nucleon is lost by annihilation — are due to the limited mass resolution. The overall feature of the correlations shows the typical liquid-drop nature of the fission process, with the large width apparently due to the broad distribution of E^* of the compound nucleus after antiproton annihilation. In the cases of U and Th the slight curvature of the mass correlation plots indicates a small contribution of asymmetric mass division which is typical for low energy fission. This effect is not evident for Bi. Outside the boundaries of the general correlation, there are a few events at the lower-left parts. The $M_{\rm tot}$ values of these events are extremely small and may be due to other processes rather than to binary fission. The energy and velocity correlations in Figs. 6 and 7 show no remarkable substructure but only the typical broad distribution. Note that the velocity correlation is much stronger than the energy correlation. The effect of the energy and time resolutions on the width of the distributions is negligible in these cases. With lower target mass the average energy becomes lower while the average velocity stays more or less constant.

C. Correlation between the total kinetic energy and the total mass of fission fragments

The dependence of the average total kinetic energy $\overline{\rm TKE}$ of the fragments on their total mass $M_{\rm tot}$ is shown in Fig. 8. The $\overline{\rm TKE}$ value decreases as $M_{\rm tot}$ is reduced. Such a behavior is explained by a well-known regularity in fission physics [12]: The kinetic energy of fission fragments is mainly defined by the energy of their Coulomb repulsion at the scission point (the contribution of the prescission kinetic energy of the fragments to the $\overline{\rm TKE}$ value is not larger than 10%). As a result, the $\overline{\rm TKE}$ value grows linearly with $Z_0^2/A_0^{1/3}$ and the $\overline{\rm TKE}$ value is larger for heavy compound nuclei; here, Z_0 is the number of protons and A_0 the number of nucleons in the residual nucleus after the cascade.

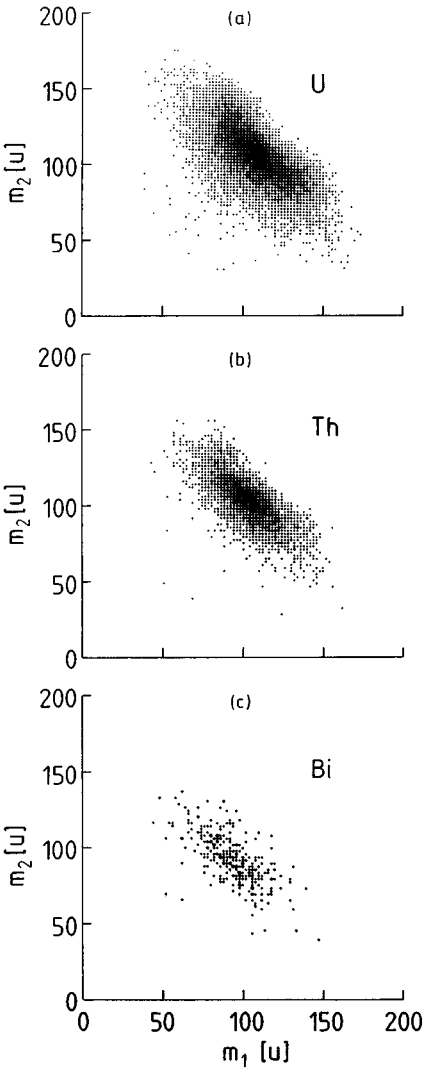

FIG. 5. Experimental mass correlations of two coincident fragments from the reactions (a) ^{238}U($\bar{p},f$), (b) ^{232}Th($\bar{p},f$) and (c) ^{209}Bi($\bar{p},f$).

The calculation of TKE agrees reasonably well with experiment (see Fig. 8) for small values of the total mass loss, $\Delta m \leqslant 30$, i.e., in the region of moderate excitation energy of the compound nucleus, $E^* \leqslant 220$ MeV, but the calculated $\overline{\rm TKE}$ values lie about 10–20 % higher than the experimental ones in the region of $30 \leqslant \Delta m \leqslant 80$ (i.e., $220 \leqslant E^* \leqslant 600$ MeV). This discrepancy may be attributed to the scission shapes being more compact in the diffusion model than in reality for fission of hot compound nuclei. The diffusion model [12] calculates the potential deformation energy of

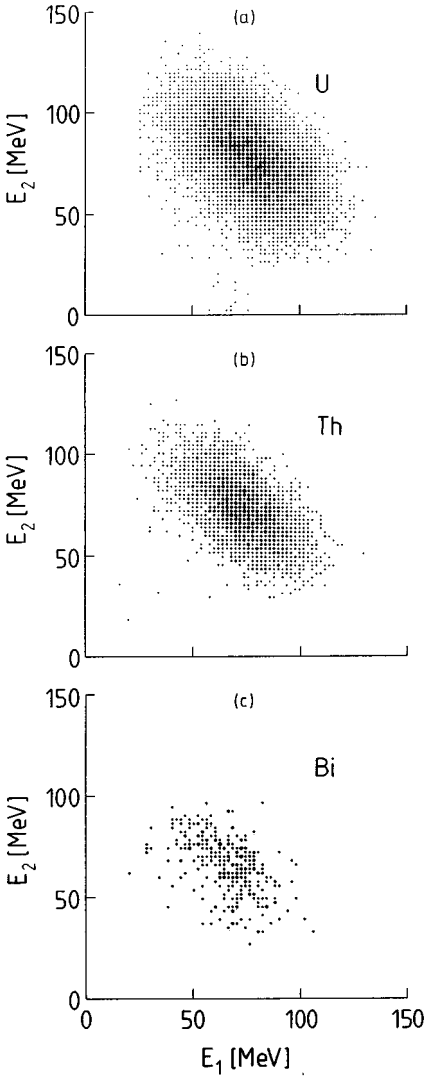

FIG. 6. Experimental kinetic energy correlations of two coincident fragments from the reactions (a) ^{238}U($\overline{p},f$), (b) ^{232}Th($\overline{p},f$), and (c) ^{209}Bi($\overline{p},f$).

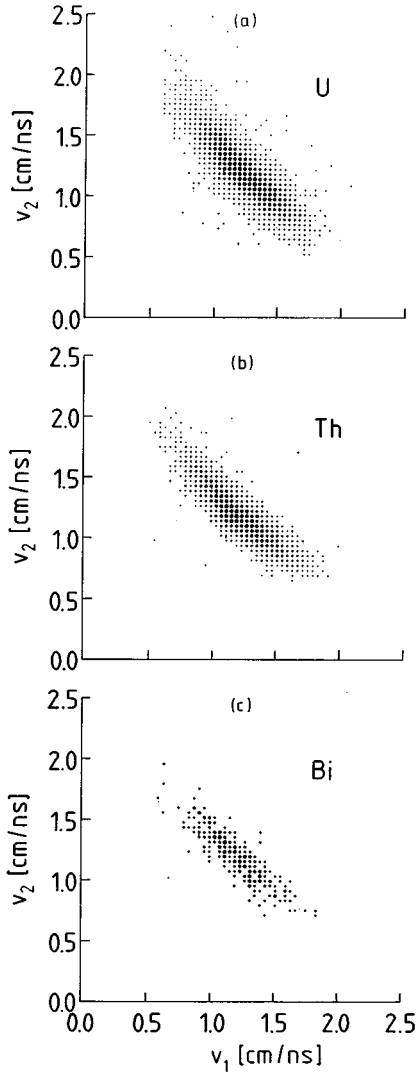

FIG. 7. Experimental velocity correlations of two coincident fragments from the reactions (a) ^{238}U(p,f), (b) ^{232}Th($\overline{p},f$), and (c) ^{209}Bi($\overline{p},f$).

fissioning nuclei using the liquid-drop model which does not take into account the temperature dependence of its parameters. The global liquid-drop properties of hot nuclei, however, are considerably different from those of cold nuclei [13,14] (in particular, a hot nucleus has a larger radius and a larger diffuse layer than a cold one). If we would take into account such thermal effects in the diffusion model, then nuclear shapes at the scission point would be less compact and, hence, the TKE of the fission fragment would be smaller.

D. Effect of particle evaporation on TKE and velocity of fission fragments

The discrepancy between calculation and measurement of TKE as a function of Δm may, however, also indicate that the enhanced number of prescission particles affects TKE seriously, as is often observed in heavy-ion reactions [7]. We note that the slope in Fig. 8 becomes steeper as more nucleons are missing in the region $\Delta m \geq 30$. As discussed in Sec. II, this indicates that more charged particles are evaporated before scission than is calculated with our model. Note that we are concerned about the slope and not the TKE value itself, which means that the temperature effect mentioned in the previous section has only minor consequences.

It is advantageous to examine the behavior of the fragment velocity and thus $d\overline{v}_{\rm rms}/dM_{\rm tot}$. The measured $\overline{v}_{\rm rms}$ data are shown in Fig. 9 for the three targets as a function of $M_{\rm tot}$. The slight increase of $\overline{v}_{\rm rms}$ with decreasing $M_{\rm tot}$ (i.e., increasing Δm) is clearly visible. The $d\overline{v}_{\rm rms}/dM_{\rm tot}$ values at $\Delta m \approx 26$ are about 6×10^{-4}, 6×10^{-4}, and 1.4×10^{-3} cm/ns nucleon for U, Th, and Bi, respectively. Note that the slope for Bi is twice as large as that for U or Th. The fission probability of Bi is much smaller than that of U and Th [15]. This implies that a comparatively larger number of neutrons than charged particles is emitted before scission of Bi, compared with U or Th.

An estimate of what the particle evaporation before and after scission means to $\overline{v}_{\rm rms}$ can be obtained by comparing experimental $\overline{v}_{\rm rms}$ values with the following extreme cases: (1) all evaporations take place after scission, (2) all evaporations take place before scission, and (3) dissipative effects

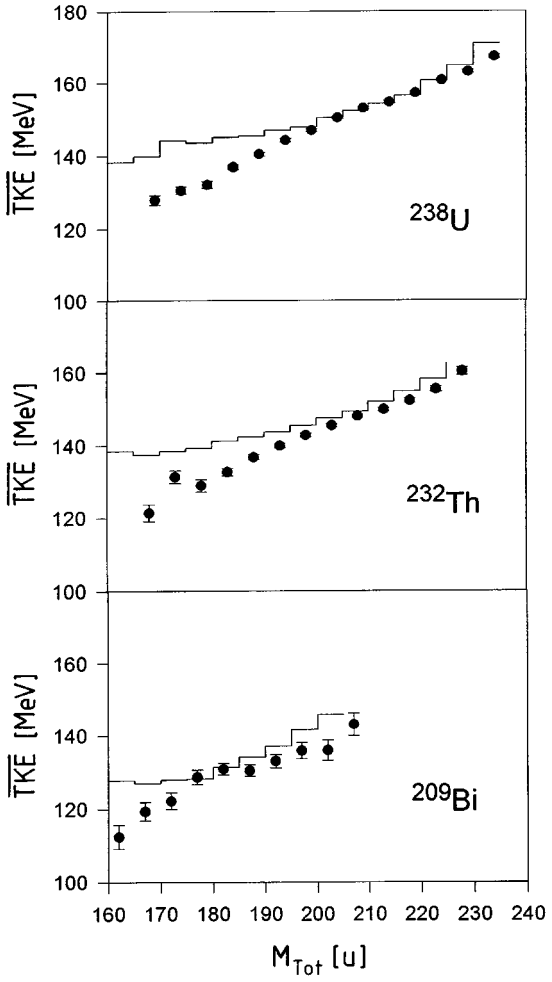

FIG. 8. Averaged values of the total kinetic energy $\overline{\mathrm{TKE}}$ as a function of the total mass M_{tot} of fission fragments for $\overline{p}$-induced fission for ^{238}U (upper part), ^{232}Th (middle part), and ^{209}Bi (lower part). Data points, experimental results of this work; histogram, calculated results.

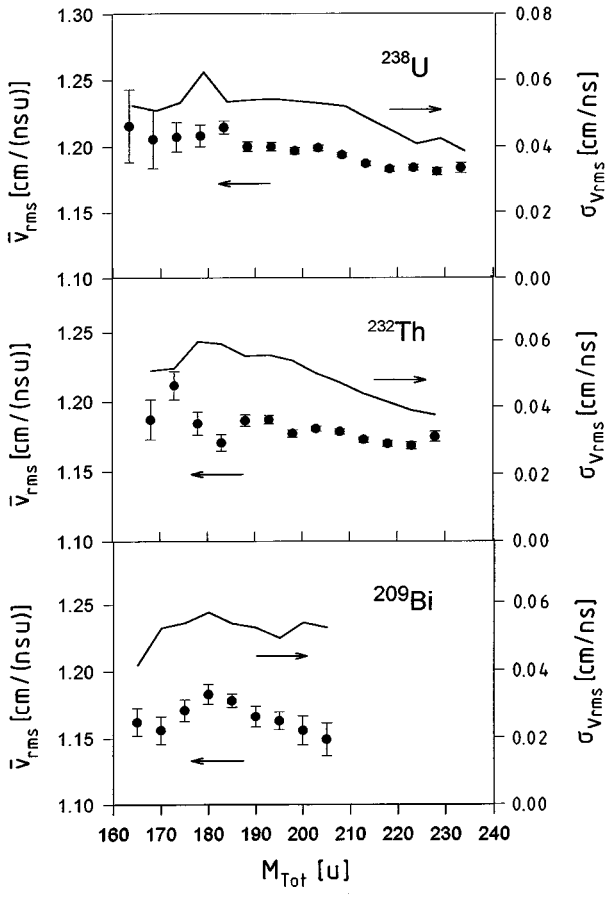

FIG. 9. Measured average root mean square velocity of fission fragments $\overline{v}_{\mathrm{rms}}$ (solid circles) and width $\sigma_{v_{\mathrm{rms}}}$ (solid curves) of the v_{rms} distribution as a function of the total mass M_{tot} for (a) ^{238}U, (b) ^{232}Th, and (c) ^{209}Bi.

play no role (the number of evaporated nucleons is the one given by Fig. 3). If one tries to be more realistic, one can assume that three neutrons are evaporated from the fission fragments due to the deformation energy. Let us further assume that the number of evaporated charged particles before scission is given by Fig. 3 for case (2). Then the average charge and mass of the fissioning nucleus can easily be obtained from the INC and statistical evaporation calculations (Figs. 2 and 3) for each case as a function of Δm. Now Eq. (5) can be used for calculating $\overline{v}_{\mathrm{rms}}$ for each case. The results are shown in Fig. 10 together with the measured values for U. It is understandable that $\overline{v}_{\mathrm{rms}}$ is almost constant in case (1), since the effects of the cascade emission of protons and neutrons approximately cancel [Figs. 2 and 4(b)], and the average velocities of the fragments will not be changed by evaporation from the fragments. In the other extreme case, $\overline{v}_{\mathrm{rms}}$ increases drastically with increasing excitation energy as a result of the evaporation of many neutrons. In the case of the statistical calculation, the trend is even reversed owing to the fact that charged-particle evaporation becomes more and more probable as E^* becomes larger (Fig. 3). Note that none of these curves are similar to the measured curve. A comparison between the calculation for case (3) and the measured values is very instructive. At small Δm the $\overline{v}_{\mathrm{rms}}$ values agree, which indicates the validity of both experimental and theoretical $\overline{v}_{\mathrm{rms}}$ values. At a mass loss $\Delta m \approx 26$, however, the difference is about 0.015 cm/ns. According to Fig. 4(b), this is a consequence of the evaporation of roughly four additional neutrons before scission, compared to the statistical calculation. With larger mass loss the difference becomes even larger.

It was mentioned in the previous sections that the total kinetic energy of hot nuclei may be reduced due to the thermal effect. Therefore, it may be dangerous to calculate the exact numbers of prescission and postscission particles from the correlation between $\overline{v}_{\mathrm{rms}}$ and M_{tot}. The comparison in Fig. 10 of the experimental values with the ones calculated for the three different cases shows at least qualitatively that the number of prescission nucleons is enhanced at high excitation energies.

E. Correlation between the momentum of the compound nucleus or of the fission fragments and the total mass

Figure 11 demonstrates the correlation between the momentum P of the fissioning nucleus (calculated from fragment momenta and folding angle) and the mass loss Δm of

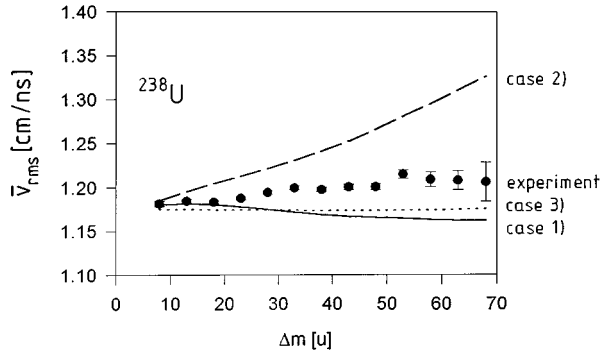

FIG. 10. $\overline{v}_{\rm rms}$ as a function of Δm calculated for the three cases discussed in the text:evaporation only after scission (solid line), all evaporation before scission (dashed line), and statistical calculation (dotted line), together with the experimental data points for ^{238}U.

the fission fragments. The average momentum $\overline{P}$ increases with mass loss Δm (i.e., with the excitation energy of the compound nucleus E^*). Such behavior was predicted in Ref. [16]: The more the collisions that take place in the intranuclear cascade, the higher are the values of excitation energy E^* and momentum P acquired by the compound nucleus. The values of P and Δm are changed as a result of subsequent evaporation from the compound nucleus and from the fission fragments, but this effect does not modify the general shape of the curve. The calculated correlation, which takes into account the evaporation effect, is in reasonable agreement with the experiment in a wide range of Δm, except for small Δm values. It should be noted that the experimental correlation is not corrected for the spectrometer resolution. In principle the momentum should be zero at $\Delta m = 0$, but due to the finite resolution in mass, energy, and angle, the momentum tends to be always larger than the real value at $\Delta m \approx 0$; note that this effect is most pronounced at $\Delta m = 0$. Taking this fact into account, the experimental correlation supports the calculated results even in the low-Δm domain.

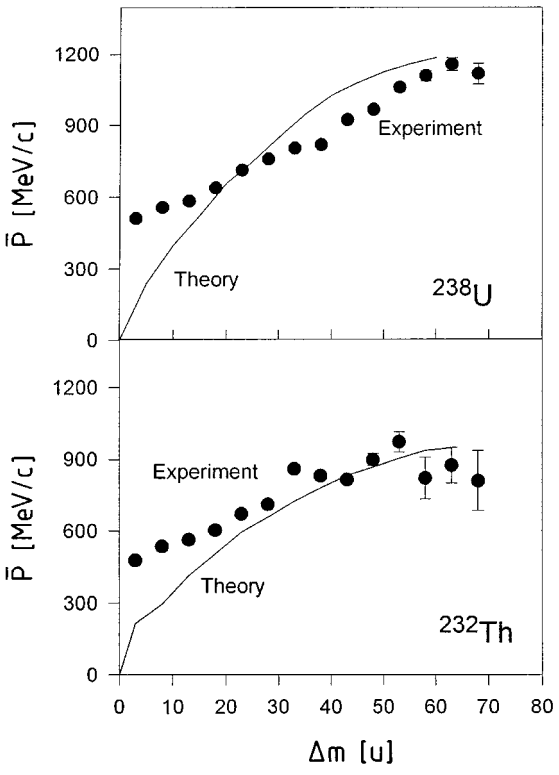

FIG. 11. Average momentum $\overline{P}$ of the fissioning nucleus as a function of the mass loss Δm of fission fragments for $\overline{p}$−induced fission of ^{238}U (upper part) and ^{232}Th (lower part). Data points, experimental results of this work; histogram, calculated results.

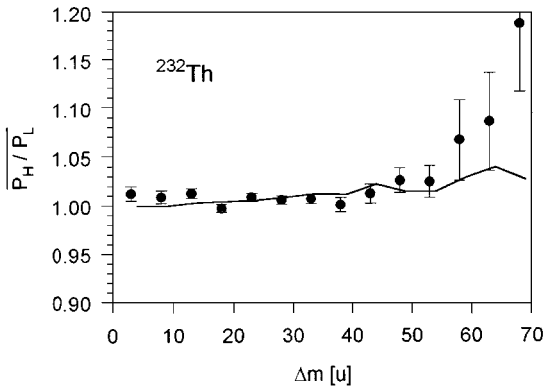

FIG. 12. Average values of the momentum ratio $\overline{P_H/P_L}$ as a function of the mass loss Δm for $\overline{p}$-induced fission of ^{232}Th. Data points, experimental results of this work; solid line, calculated results.

The correlation between the momentum ratio of heavy and light fragments P_H/P_L and the mass loss Δm is another interesting topic. The following expression for the average value of this ratio has been deduced in Ref. [17]:

$$\overline{P_H/P_L} = 1 + \overline{\Delta m^L_{af}/M_L} - \overline{\Delta\ m^H_{af}/M_H} + \text{ higher order terms}, \tag{6}$$

where M and $\Delta m_{\rm af}$ are the mass and mass loss after scission of the heavy (H) and light (L) fragment. The excitation energy of the compound nucleus will be shared between the two fission fragments proportionally to their masses if scission takes place after thermalization, and then $\overline{\Delta m^H_{af}/M_H} \approx \overline{\Delta m^L_{af}/M_L}$ and $\overline{P_H/P_L} \approx 1$. Consequently, the $\overline{P_H/P_L}$ ratio may be used as a measure of the degree of thermalization in the fissioning nucleus.

A comparison of the calculated and experimental dependence of the $\overline{P_H/P_L}$ ratio on Δm is shown in Fig. 12 for the Th target. As one would expect, the $\overline{P_H/P_L}$ ratio is close to unity for most Δm values and theory is in good agreement with experiment. The calculated $\overline{P_H/P_L}$ ratio is slightly larger than 1.0 for $\Delta m \geqslant 30$ (i.e., for the fission of hot compound nuclei) due to the increasing role of evaporation of charged particles (mainly α particles). The experimental $\overline{P_H/P_L}$ ratios at $\Delta m \geqslant 60$, however, are larger than the theoretical ones. The discrepancy between theory and experiment, visible in Fig. 12, may indicate fast cracking of the nucleus into two fragments before thermal equilibration or breakup of the nucleus into several fragments starts to play a role. The first process (called cleavage) was observed in an 11.5 GeV proton-induced-fission experiment [18], but it

seems that such a mechanism is unlikely in the case of nuclear absorption of antiprotons with ''zero'' primary momentum. The second process was investigated in Ref. [19]. It was predicted that the explosive breakup of hot residual nuclei into several fragments (called multifragmentation) may be observed with finite (rather small) probability in $\bar{p}$-nucleus annihilation. Breakup of the nucleus into a small number of fragments may take place in $\bar{p}$-nucleus annihilation at rest, either as quasievaporation (i.e., breakup into a large fragment and one or two small fragments) or as quasifission (i.e., breakup into two fragments with approximately equal masses and one or two small fragments).

IV. SUMMARY

Fission of heavy nuclei induced by stopped antiprotons was investigated experimentally in a systematic way both in the present and in a previous [5] publication. Both inclusive characteristics of the fission fragments and correlations between them were measured. The data were discussed in the framework of the dynamical statistical approach which takes into account all stages before, during, and after $\bar{p}$-induced fission (atomic cascade, intranuclear cascade, evaporation cascade, fission of the compound nucleus, evaporation from the fission fragments). The approach in general gives a good description of the experimental data. Some discrepancies, however, indicate that the diffusion model, which describes the dynamics of descent of the fissioning nucleus from saddle to scission point, needs to be improved. The influence of thermal effects on the surface of the deformation energy, the emission of neutrons and other particles during descent from saddle to scission point, and the temperature dependence of the nuclear viscosity coefficient must be taken into account. It is possible to do this in the framework of the diffusion model based on the Langevin equation [20–22].

The examination of the correlation data, especially the correlations of total kinetic energy and velocity to mass loss, indicates that a larger number of prescission particles is evaporated than is expected from the statistical evaporation model.

ACKNOWLEDGMENTS

We wish to thank P. Maier-Komor and K. Nacke for the target preparation, H. Hagn, P. Stoeckel, and F. Fridgen for technical help, D. Bowman, P. David, E. Gawathas, J. Jastrzebski, W. Kurcewicz, J. Lieb, W. Lynch, B. Wright, and K. Ziock for collaboration, and G.D. Adeev, A.S. Botvina, Ye.S. Golubeva, D. Hilscher, N.I. Pischasov, and O.I. Serdyuk for discussions. The LEAR team provided an excellent antiproton beam. Two of us (A.S.I. and M.V.M.) express gratitude to the Technical University of Munich for the warm hospitality and to the Deutsche Forschungsgemeinschaft, Bonn, for support, and one of us (H.S.P.) acknowledges travel support from the NATO Scientific Affairs Division. The work was supported by the German Bundesministerium für Forschung und Technologie, Bonn, and the Beschleunigerlaboratorium der Universität und Technischen Universität München.

[1] J.O. Newton, Sov. J. Part. Nucl. **21**, 349 (1990).
[2] B.L. Gorshkov, A.I. Il'in, B.Yu. Sokolovskii, G.E. Solyakin, and Yu. A. Chestnov, JETP Lett. **37**, 72 (1983).
[3] S. Bohrmann, J. Hüfner, and M.C. Nemes, Phys. Lett. **120B**, 59 (1983).
[4] S.B. Kaufman, Nucl. Phys. **A471**, 163c (1987).
[5] P. Hofmann, A.S. Iljinov, Y.S. Kim, M.V. Mebel, H. Daniel, P. David, T. von Egidy, T. Haninger, F.J. Hartmann, J. Jastrzebski, W. Kurcewicz, J. Lieb, H. Machner, H.S. Plendl, G. Riepe, B. Wright, and K. Ziock, Phys. Rev. C **49**, 2555 (1994).
[6] Y.S. Kim, P. Hofmann, H. Daniel, T. von Egidy, T. Haninger, F.J. Hartmann, and M.S. Lotfranaei, Nucl. Instrum. Methods A **329**, 403 (1993); P. Hofmann, Ph.D. thesis, Technische Universität München, 1992; Y.S. Kim, Ph.D. thesis, Technische Universität München, 1992.
[7] D. Hilscher and H. Rossner, Ann. Phys. (Paris) **17**, 471 (1992); D. Hilscher, Nucl. Phys. **A471**, 77c (1987).
[8] L.P. Remsberg, F. Plasil, J.B. Cumming, and M.L. Perlman, Phys. Rev. **187**, 1597 (1969).
[9] N. Metropolis, R. Bivins, M. Strom, and J.M. Miller, Phys. Rev. **110**, 204 (1958).
[10] I. Dostrovsky, P. Rabinowitz, and R. Rubins, Phys. Rev. **111**, 1659 (1958).
[11] V.E. Viola, Jr., Nuclear Data Tables A **1**, 391 (1966).
[12] G.D. Adeev, A.S. Botvina, A.S. Iljinov, M.V. Mebel, N.I. Pischasov, and O.I. Serdyuk, Report No. INR-816/93, Moscow, 1993.
[13] A.S. Iljinov, E.A. Cherepanov, and S.E. Chigrinov, Z. Phys. A **287**, 37 (1978).
[14] U. Mosel, in *Heavy Ion Collisions*, edited by R. Bock (North-Holland, Amsterdam, 1980), Vol. 2, p. 275.
[15] W. Schmid, P. Baumann, H. Daniel, T. von Egidy, F.J. Hartmann, P. Hofmann, Y.S. Kim, H.H. Schmidt, A.S. Iljinov, M.V. Mebel, D. Hilscher, D. Polster, and H. Rossner, Nucl. Phys. **A569**, 689 (1994).
[16] A.S. Iljinov, V.I. Nazaruk, and S.E. Chigrinov, Nucl. Phys. **A382**, 378 (1982).
[17] Yu.A. Chestnov, A.V. Kravtsov, B.Yu. Sokolovskii, and G.E. Solyakin, Sov. J. Nucl. Phys. **45**, 11 (1987).
[18] B.D. Wilkins, S.B. Kaufmann, E.P. Steinberg, J.A. Urbon, and D.J. Henderson, Phys. Rev. Lett. **43**, 1080 (1979).
[19] Ye.S. Golubeva, A.S. Iljinov, A.S. Botvina, and N.M. Sobolevsky, Nucl. Phys. **A483**, 539 (1988).
[20] I.I. Gonchar, G.I. Kosenko, N.I. Pischasov, and O.I. Serdyuk, Sov. J. Nucl. Phys. **55**, 514 (1992).
[21] I.I. Gonchar and P. Fröbrich, Nucl. Phys. **A551**, 495 (1993).
[22] T. Wada and N. Carjan, Nucl. Phys. **A538**, 283c (1992).